Spin splitting of the excited-state subband in GaAs-$Al_{0.3}Ga_{0.7}As$ asymmetric two-layer systems

Y. Takagaki, K.-J. Friedland, R. Hey, and K. H. Ploog
Paul-Drude-Institut für Festkörperelektronik, Hausvogteiplatz 5-7, 10117 Berlin, Germany
(Received 14 February 2002; published 9 July 2002)

We track the variation of the Landau-level filling factors for the quantization of the Hall resistance in unbalanced double-quantum-well structures when the electron density is a controlled parameter. We observe that the filling factors associated with adjacent quantum Hall states differ by three for two or more consecutive quantum Hall transitions. The anomalous filling-factor increment results from simultaneous depopulations of a spin-degenerate Landau level of the ground-state subband and a spin-polarized Landau level of the excited-state subband. The locking of the topmost Landau levels to the Fermi level gives rise to the phenomenon in which the Zeeman splitting of the excited-state subband can be mistaken to be enormous enough to match the Landau-level separation of the ground-state subband. The temperature dependence of the quantum Hall states evidences, however, that the exchange enhancement of the g factor for the excited-state subband is rather similar to that for the ground-state subband.

DOI: 10.1103/PhysRevB.66.035309 PACS number(s): 73.43.Qt, 73.50.Jt

I. INTRODUCTION

In spite of the small g factor of GaAs ($g=-0.44$), the Shubnikov–de Haas (SdH) oscillation in the longitudinal resistivity ρ_{xx} and the quantum Hall effect in the Hall resistivity ρ_{xy} of a two-dimensional electron gas (2DEG) readily develop features arising from lifting the spin degeneracy. The g factor of the 2DEG is strongly enhanced from the bulk value because of the exchange effect among electrons in a Landau level.[1] In a magnetic field B, the Zeeman splitting produces a situation where the number of electrons with up spin is larger than that with down spin. The disorder broadening of the Landau levels in typical GaAs-$Al_xGa_{1-x}As$ heterostructures is considerably greater than the Zeeman energy $g\mu_B B$, where μ_B is the Bohr magneton, so that both of the spin states would be partially occupied. However, the exchange effect prefers having only the up-spin branch occupied, as the Coulomb repulsion is reduced owing to the Pauli exclusion principle.[2]

The magnitude of the spin splitting has been evaluated experimentally using, for example, the tilt-angle method.[1] The Zeeman splitting depends on the total magnetic field, whereas the magnetic-field component $B_\perp$ perpendicular to the 2DEG plane determines the Landau-level separation $\hbar\omega_c$, where $\omega_c=eB_\perp/m$ is the cyclotron frequency. Taking advantage of this behavior, the energy separation between the up- and down-spin states can be estimated by identifying the tilt angles at which the spin-split states from various Landau levels overlap. It was reported that the effective g factor g^* could be an order-of-magnitude larger than the bulk value.[3,4]

In this paper, we direct our attention to the spin splitting of the excited-state subband in an asymmetric two-layer system instead of the ground-state subband. The magnetotransport properties in this system are distinguished by the disappearance of the quantum Hall states at certain values of the Landau-level filling factor ν and the quantization of ρ_{xy} at some odd integer values of ν.[5,6] These phenomena are accompanied by a peculiarity that may be interpreted to mean that the spin splitting of the excited-state subband is as large as the Landau-level separation of the ground-state subband. We demonstrate that this nominal evidence for the giant g^* of the excited-state subband is merely a consequence of the pinning of the Landau levels to the Fermi level and that the g-factor enhancements are comparable for the ground- and excited-state subbands.

II. SAMPLES

We investigate the magnetotransport properties in asymmetric double-quantum-well structures that were grown by molecular-beam epitaxy. The potential profile for electrons is depicted in the inset of Fig. 1. Two GaAs quantum wells having the thicknesses of 15 and 10 nm are separated by an $Al_{0.3}Ga_{0.7}As$ barrier with the thickness of 6 nm. The ground- and excited-state subbands localize in the wide and narrow

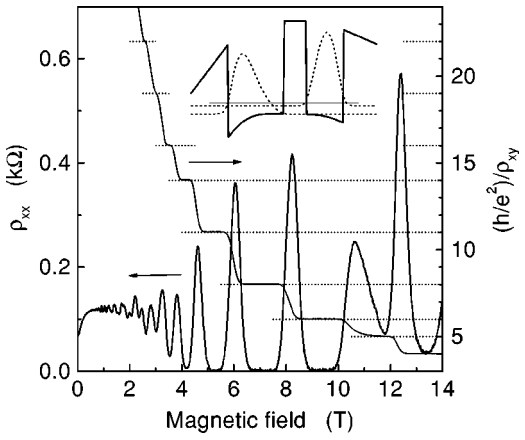

FIG. 1. Magnetic-field dependencies of the longitudinal resistivity ρ_{xx} and the inverse of the Hall resistivity ρ_{xy} normalized by the conductance quantum e^2/h in heterostructure 1 at $T=0.3$ K. The inset shows the profile of the conduction-band edge around the GaAs-$Al_{0.3}Ga_{0.7}As$ quantum wells. The probability distributions and the threshold energies of the bottom two subbands are illustrated by the dotted lines. The thin solid line indicates the Fermi level.

quantum wells, respectively. Electrons are supplied by two δ-doping layers. In heterostructure 1, a principal δ-doped plane with the Si concentration of 2×10^{16} m^{-2} is placed adjacent to the wide quantum well with a spacer layer thickness of 10 nm. A subsidiary δ-doped plane with the Si concentration of 6×10^{15} m^{-2} is embedded in the $Al_{0.3}Ga_{0.7}As$ layer in the vicinity of the narrow quantum well at a distance of 20 nm. In heterostructure 2, the Si density for the subsidiary doping is 4×10^{15} m^{-2}.

The quantum-well structures were processed into Hall bars with Ohmic contacts which connect both wells. The samples were mounted in a ^{3}He cryostat and magnetoresistivity measurements were performed using low-frequency lock-in techniques. The magnetic field was applied normal to the Hall bar, i.e., $B_\perp = B$. The electron densities were controlled using the persistent photoconductivity effect. We employed a red light-emitting diode to illuminate the samples.

III. EXPERIMENTAL RESULTS

Figure 1 shows the magnetic-field dependencies of ρ_{xx} and ρ_{xy} in heterostructure 1 at a temperature $T=0.3$ K. The irregularity of the SdH oscillation amplitude indicates that the population threshold of the excited-state subband is below the Fermi level. In addition, a positive magnetoresistance and a kink in ρ_{xy} are exhibited near zero magnetic field as a consequence of the presence of the two kinds of carriers.[7,8] We have analyzed these low-B transport properties to determine the electron mobilities, see the Appendix. The values we obtained for the ground- and excited-state subbands are, respectively, $\mu_1=3.0$ m^2/Vs and $\mu_2=17$ m^2/Vs with the electron densities of the two subbands $n_1=10.2\times10^{15}$ m^{-2} and $n_2=3.6\times10^{15}$ m^{-2}. For heterostructure 2, we obtain $\mu_1=6.6$ m^2/Vs and $\mu_2=11$ m^2/Vs when $n_1=9.4\times10^{15}$ m^{-2} and $n_2=4.9\times10^{15}$ m^{-2}. Because of the roughly comparable mobilities of the two subbands, the low-B anomalies are much less pronounced in heterostructure 2 (not shown).

In Fig. 1, we have normalized the inverse of ρ_{xy} by the conductance quantum e^2/h so that one can clearly see that the Hall resistance is quantized almost exactly at integer fractions. These integer values are unevenly spaced. The filling factor changes either by one, two, or three between adjacent quantum Hall states. The electron mobilities in the heterostructures are relatively low. Thus, the Landau levels are expected to be spin degenerate, at least, for the ground-state subband,[9] leading to $\Delta\nu=2$. The case of $\Delta\nu=1$ implies that the spin degeneracy is lifted for the Landau level which is being magnetically depopulated. The case of $\Delta\nu=3$ suggests a degeneracy of a spin-unresolved Landau level and a spin-polarized Landau level.

As a large number of electrons are distributed to the excited-state subband, both of the subbands generate peaks in ρ_{xx} with indistinguishable magnitudes.[10,11] In order to identify the parent subband of the magnetoresistance peaks, we plot in Fig. 2(a) the position of the peaks in B as a function of the total electron density n_1+n_2. For each domain surrounded by the magnetoresistance peaks, ν deduced from the quantized value of ρ_{xy} is indicated. The peaks originating from a common subband shift in B in a similar fashion when the electron density is varied. Therefore, the Landau-level indices can be assigned unambiguously. Here, Gi and Ei refer to the ith Landau level of, respectively, the ground- and excited-state subbands and arrows stand for the two spin orientations.

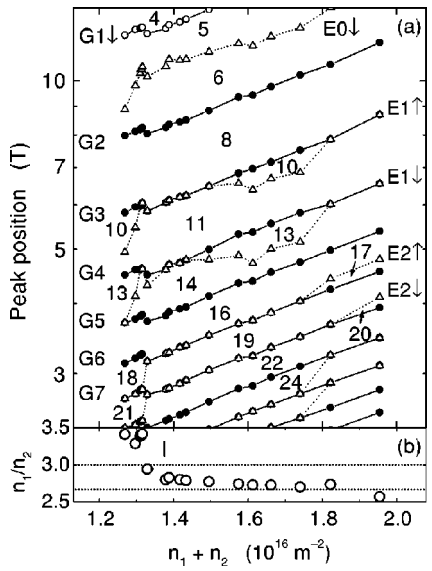

FIG. 2. (a) Phase diagram of the quantum Hall effect in heterostructure 1. The position of the peaks in ρ_{xx} is plotted as a function of the total sheet electron density n_1+n_2. The circles and the triangles represent the Landau levels associated with the ground- and excited-state subbands, respectively. The filled and open symbols indicate that the state is spin degenerate and spin polarized, respectively. The Landau-level filling factor is indicated for each domain surrounded by the peaks. The ith Landau level of the ground- and excited-state subbands is labeled Gi and Ei, respectively. Arrows stand for the two spin orientations. (b) Ratio between the electron densities n_1 and n_2 in the two subbands. The dotted lines indicate $n_1/n_2=3$ and 8/3. The bar indicates n_1+n_2 for the data in Fig. 1.

Having the assignment accomplished in this manner, we immediately make an observation: The Landau levels associated with the ground-state subband are spin degenerate, except for G1, which shows up at the highest magnetic field, whereas all the Landau levels associated with the excited-state subband are fully spin polarized. It then becomes apparent that $\Delta\nu=3$ arises from an overlap of two Landau levels, each of which originates from the ground- and excited-state subbands. The complete spin polarization is intact even when the temperature is raised to 1.5 K. These trends are found also in heterostructure 2 as presented in Fig. 3. We note that the ratio n_1/n_2 remains in the range of 1.9 $\sim$2.2 in heterostructure 2.

The anomalous filling-factor increment $\Delta\nu=3$ around $\nu=11$ and 19 in heterostructure 1 takes place successively for two quantum Hall transitions. Amazingly, heterostructure 2 exhibits the behavior $\Delta\nu=3$ for six transitions in a row between $\nu=6$ and $\nu=24$. In view of the analogy to the tilt-angle method, this could imply that the Zeeman splitting of the excited-state subband equals the energy separation of the Landau levels of the ground-state subband. Such an interpre-

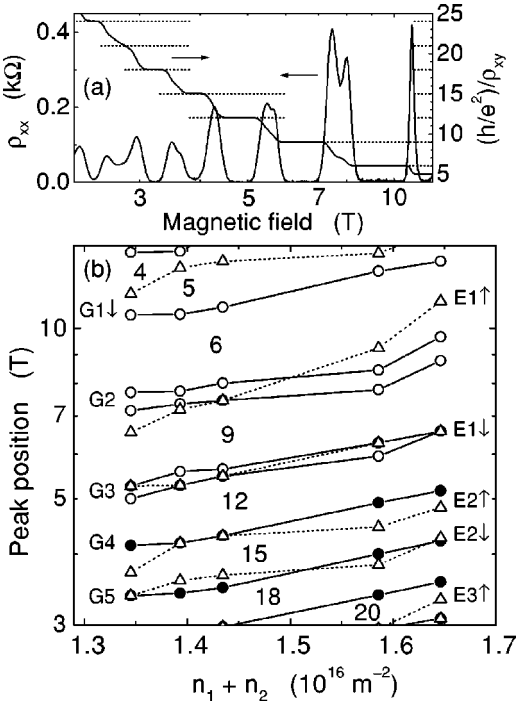

FIG. 3. (a) Longitudinal resistivity ρ_{xx} and inverse Hall resistivity ρ_{xy}^{-1} in heterostructure 2 at $T=0.3$ K. (b) Position of the peaks in ρ_{xx}. The Landau-level filling factor is indicated for major quantum Hall states. The ith Landau level associated with the ground- and excited-state subband is indicated by Gi (solid lines) and Ei (dotted lines), respectively.

tation $g^*\mu_B B \approx \hbar\omega_c$ yields the gigantic value of about 30 for g^*. However, the temperature dependence of the quantum Hall states reveals that g^* of the excited-state subband is rather comparable to that of the ground-state subband.

The circles in Fig. 4 show the amplitude $\Delta\rho=\rho_{xx}-\rho_0$ of

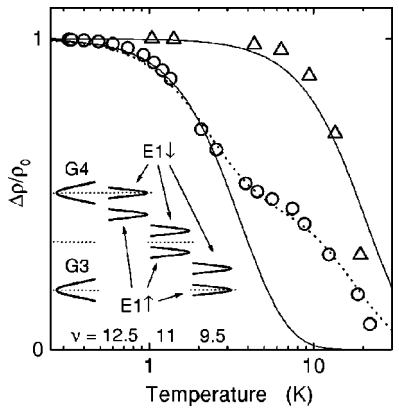

FIG. 4. Magnitude of the Shubnikov–de Haas oscillation $\Delta\rho$ normalized by the background resistivity ρ_0 in heterostructure 1. The circles correspond to the quantum Hall state at $\nu=11$ in Fig. 1. The triangles show the temperature dependence for the quantum Hall state at $\nu=8$ when the electron density is the lowest in Fig. 2. The lines are theoretical fits. The inset shows the density-of-states diagram. The position of the two spin states of the Landau level E1 is illustrated with respect to the Landau levels G3 and G4 at $\nu=12.5$, 11, and 9.5. The Fermi level is indicated by the dotted lines.

the SdH oscillations normalized to the background resistivity ρ_0 for the quantum Hall state at $\nu=11$ in Fig. 1. The energy gap E_g is deduced using the relation $\Delta\rho \propto \Lambda \sinh\Lambda$ with $\Lambda = 2\pi^2 k_B T/E_g$. The fit to the experimental data is shown by the solid line, yielding $E_g=2.4$ meV. This value is considerably smaller than $\hbar\omega_c=9.2$ meV at $B=5.3$ T. If we regard the energy gap as the spin splitting of the Landau level E1, we obtain $g^*=7.8$, which compares well with the values found for the ground-state subband.[3,4] To check the reliability of the estimate of E_g, we have also examined the temperature dependence of $\Delta\rho/\rho_0$ at $\nu=8$ at the lowest electron density, $n_1+n_2=12.7\times10^{15}$ m^{-2} (triangles). The resistivity peaks associated with the excited-state subband emerge at this electron density at magnetic fields significantly away from the peaks that delineate the $\nu=8$ quantum Hall region, so that E_g is expected to correspond to the separation between the Landau levels G2 and G3. We indeed obtain $E_g=14$ meV, which is in reasonable agreement with $\hbar\omega_c=11.6$ meV at $B=6.7$ T. As the excited-state subband supplies the quantum Hall state at $\nu=11$ with the small energy gap, its temperature dependence is, in fact, dominated above 3 K by the ground-state subband. Assuming that the contributions from the two subbands are additive with identical magnitudes, a better theoretical fit can be made as indicated by the dotted line. From the low- and high-temperature behaviors, $E_g=1.7$ and 11.3 meV are extracted, respectively. These values are quite reasonable for the spin splitting of the excited-state subband, corresponding to $g^*=5.5$, and the Landau-level separation of the ground-state subband.

The activation energy Δ is derived using the formula $\rho_{xx}=\rho_0\exp(-\Delta/2k_BT)$. For the quantum Hall state at $\nu=11$ in Fig. 1, Δ is estimated to be 0.38 meV, which is equivalent to 4.4 K. We obtain $\Delta=0.82$ meV for the quantum Hall state at $\nu=8$ in Fig. 3(a). It is known that Δ is smaller than E_g. The difference corresponds to the disorder broadening of the Landau levels. The result $\Delta \ll E_g$ is consistent with the relatively low electron mobilities in the quantum wells.

IV. DISCUSSION

The most important characteristic of the asymmetric two-layer system for understanding the aforementioned features is the crossing of the Landau levels originating from the two subbands. If the excited-state subband holds a very small number of electrons, only its lowest Landau level is relevant in high magnetic fields. In this circumstance, the bottom Landau level of the excited-state subband always crosses the Landau level of the ground-state subband in which the Fermi level initially resides along the course of the magnetic depopulation of a single Landau level.[12] Hence, the excited-state subband replaces the ground-state subband in hosting the Fermi level.

When increasing the electron occupation in the excited-state subband, the Landau-level crossing moves to larger filling factors. Eventually, some of the crossings coincide with the magnetic depopulation of the neighboring Landau levels. In the Landau-level diagram in Fig. 5, we show how the Fermi energy, which is indicated by the thick solid line,

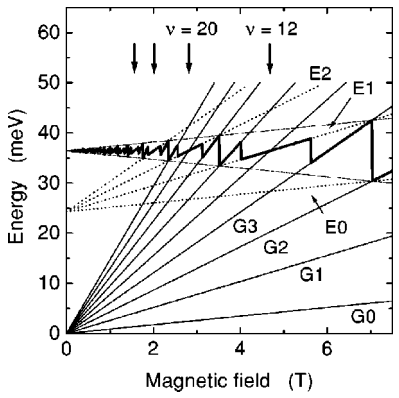

FIG. 5. Landau-level diagram in an asymmetric two-layer system when the spin splitting is ignored. The thick solid line indicates the Fermi energy when the electron densities in the ground- and excited-state subbands are 10.2 and 3.4×10^{15} m^{-2}, respectively. The thin solid lines and dotted lines show the energy of the Landau levels associated with the ground- and excited-state subbands, respectively. The position for the disappearance of the quantum Hall states due to the Landau-level crossing is indicated by the vertical arrows.

changes with the magnetic field for the case of $n_1=10.2\times10^{15}$ m^{-2} and $n_2=3.4\times10^{15}$ m^{-2}. Here, we have ignored the spin. As indicated by the arrows, the coincidence results in a vanishing Landau gap at $\nu=(2i-1)(\eta+1)=\nu_c$ with i being integers when the ratio n_1/n_2 is set to be an odd integer value η. The quantum Hall effect disappears if the Landau gap is absent.[13] Notice that the Landau gap due to the ground-state subband is unaffected by the excited-state subband at $\nu=2i(\eta+1)$.

In Fig. 2(a), a pronounced quantum Hall effect is indeed found at $\nu=8$ $(\eta=3)$. However, instead of the simple disappearance of the quantum Hall effect anticipated above, the ''vanished'' quantum Hall state at $\nu=\nu_c$ and the regular quantum Hall state at $\nu=\nu_c-2$ merge to give rise to the quantization of ρ_{xy} at $\nu=\nu_c-1$ with $\Delta\nu=3$. The hybridization is driven by the potential renormalization arising from the interlayer charge transfer.[11] While a Landau level is vacated, the electrons in this level have to be redistributed between the two subbands. However, the charge can be extracted from or added to a subband only if the density of states is finite at the Fermi level. Moreover, the changes in the Hartree potential resulting from the interlayer charge transfer have to satisfy the self-consistency of the potential. The Landau-level crossing in a real system is thus altered significantly from the noninteracting-subband model displayed in Fig. 5. The abrupt jump and the switch of the Fermi level between the two subbands, which are inevitable in the noninteracting model, are forbidden. The topmost Landau level of each subband is, therefore, required to be positioned at the Fermi level.[14]

When the two consecutive $\Delta\nu=3$ transitions take place around $\nu=11$, the spin-up and spin-down states of the Landau level E1 are aligned with respect to the Landau levels G3 and G4. As manifested by the temperature dependence, $g^*\mu_B B\ll\hbar\omega_c$ and the level E1 is sandwiched by the levels G3 and G4 when the Fermi level lies at the center of the energy gap, see the inset of Fig. 4. When ρ_{xx} develops a peak at a magnetic field weaker $(\nu=12.5)$ or stronger $(\nu=9.5)$ than that for the midgap Fermi level $(\nu=11)$, the self-consistent potential arranges itself to make, respectively, the E1$\downarrow$ or E1$\uparrow$ state overlap with the Landau level G4 or G3.

The coincidence of the spin gap of the Landau level Ei and the gap between the Landau levels G$(j-1)$ and Gj takes place at the Fermi level when $n_1/n_2=2j/(2i+1)$. As $n_1/n_2\approx2$ in heterostructure 2, the coincidence occurs for all odd integers of j. Consequently, the Landau-level locking gives rise to the behavior $\Delta\nu=3$ for all the quantum Hall transitions. In heterostructure 1, the coincidence condition is fulfilled only approximately. It should be noted that the total electron density will fluctuate with B to minimize the interlayer charge transfer.[12] The self-regulation of the electron density may be responsible for the stability of the $\Delta\nu=3$ behavior over the wide range of n_1+n_2 regardless of the small but finite deviations of the ratio n_1/n_2 from 8/3 for $\nu=11$ or 14/5 for $\nu=19$.

Despite the small difference between μ_1 and μ_2 in heterostructure 2, the complete spin polarization for the excited-state subband and the barely visible spin polarization for the ground-state subband are in striking contrast. There are several reasons that possibly account for the drastic difference. First, g^* is expected to increase monotonically with decreasing electron density.[15] Second, the disorder broadening is generally larger for higher Landau levels.[1] Third, Fogler and Shklovskii[16] have shown that the spin splitting due to the exchange enhancement of the g factor is a second-order phase transition and that the resistivity peaks associated with the two spin orientations are well separated as soon as the disorder broadening of the Landau levels becomes less than a critical value. Fourth, the potential renormalization will additionally enlarge the peak separation for the excited-state subband through the mechanism we described above.

V. CONCLUSIONS

We have studied the quantum Hall effect in asymmetric double-quantum-well structures when the ratio n_1/n_2 between the electron densities in the two subbands is approximately three or two. Over a wide range of the total electron density, the filling-factor increment is found to be three for two consecutive quantum Hall transitions when $n_1/n_2=3$ and for all the transitions when $n_1/n_2=2$. The potential renormalization associated with the interlayer charge transfer induces a hybridization of a vanished Landau gap due to the Landau-level crossing and a neighboring regular Landau gap, leading to simultaneous depopulations of a spin-degenerate Landau level of the ground-state subband and a spin-polarized Landau level of the excited-state subband. This gives rise to a behavior which can be misinterpreted to mean that the Zeeman splitting of the excited-state subband is as large as the Landau-level separation of the ground-state subband. The energy gap deduced from the temperature dependence indicates that the effective g factor for the excited-state subband is not abnormally larger than that for the ground-state subband.

ACKNOWLEDGMENTS

The authors thank A. Riedel and E. Wiebicke for technical assistance. Part of this work was supported by the Deutsche Forschungsgemeinschaft and by the NEDO collaboration program.

APPENDIX: TWO-CARRIER MODEL

We derive the formulas to determine the electron mobilities in a two-subband system. In the conventional magnetotransport measurements using a Hall bar, voltage drops are measured in the directions parallel and perpendicular to the current while a magnetic field B is applied normal to the Hall bar. The voltage drops in a single-subband system are related to the current by the resistivity tensor

$$\tilde{\rho}=\begin{pmatrix}(en\mu)^{-1} & -B/en\\ B/en & (en\mu)^{-1}\end{pmatrix}, \tag{A1}$$

where n and μ are the electron density and the mobility, respectively. The contributions from the two kinds of the carriers in the two-subband system are additive in terms of the conductivity tensor. Therefore, ρ_{xx} and ρ_{xy} in the two-subband system obey the relationship

$$\begin{pmatrix}\rho_{xx} & -\rho_{xy}\\ \rho_{xy} & \rho_{xx}\end{pmatrix}=(\tilde{\rho}_1^{-1}+\tilde{\rho}_2^{-1})^{-1}, \tag{A2}$$

where $\tilde{\rho}_i$ belongs to the subband i. To be specific, we arrive at

$$\rho_{xx}=\frac{X}{e(X^2+Y^2)}, \tag{A3}$$

$$\rho_{xy}=\frac{Y}{e(X^2+Y^2)}, \tag{A4}$$

where

$$X=\frac{n_1\mu_1}{1+(\mu_1 B)^2}+\frac{n_2\mu_2}{1+(\mu_2 B)^2},$$

$$Y=\left[\frac{n_1\mu_1^2}{1+(\mu_1 B)^2}+\frac{n_2\mu_2^2}{1+(\mu_2 B)^2}\right]B.$$

Equations (A3) and (A4) reduce to the well-known expressions

$$\rho_{xx}=\frac{1}{e(n_1\mu_1+n_2\mu_2)}, \tag{A5}$$

$$\rho_{xy}=\frac{n_1\mu_1^2+n_2\mu_2^2}{e(n_1\mu_1+n_2\mu_2)^2}B \tag{A6}$$

in the limit of $B\to 0$. In the opposite limit of large B, one finds

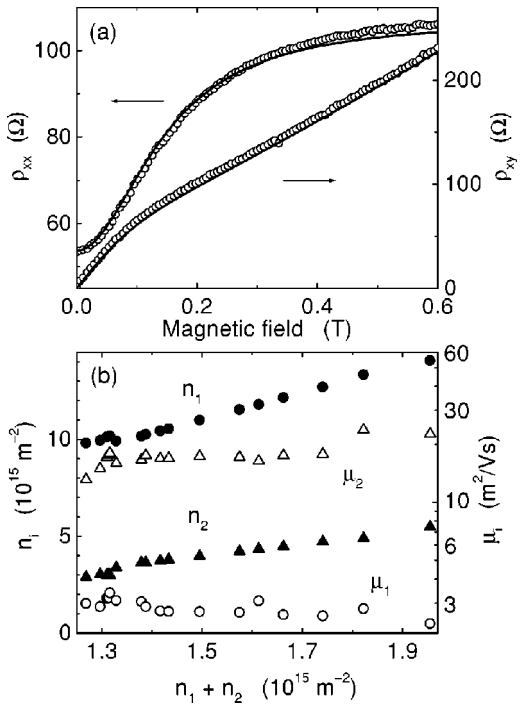

FIG. 6. (a) Longitudinal resistivity ρ_{xx} and Hall resistivity ρ_{xy} in heterostructure 1 at weak magnetic fields. The experimental data are shown by the circles. The solid lines show the theoretical fits with parameters of $\mu_1=2.6$ m^2/Vs, $\mu_2=17.8$ m^2/Vs, $n_1=12.7\times10^{15}$ m^{-2}, and $n_2=4.7\times10^{15}$ m^{-2}. (b) Electron mobility μ_i and electron density n_i of the ground-state ($i=1$) and excited-state ($i=2$) subbands vs total electron density n_1+n_2 in heterostructure 1.

$$\rho_{xx}=\left(\frac{n_1}{n_1+n_2}\right)^2\frac{1}{en_1\mu_1}+\left(\frac{n_2}{n_1+n_2}\right)^2\frac{1}{en_2\mu_2}, \tag{A7}$$

$$\rho_{xy}=\frac{B}{e(n_1+n_2)}. \tag{A8}$$

Despite the simple and phenomenological derivation of Eqs. (A3) and (A4), Eqs. (A7) and (A8) agree with the predictions from a microscopic calculation.[17]

A comparison of the theory with the experimental data is made in Fig. 6(a). The theoretical curves reproduce the experimental results remarkably well over the entire magnetic-field range. The electron densities in the two subbands are independently determined by the SdH oscillations, and so the mobilities can be, in principle, obtained solely from the transport coefficients at $B=0$. However, such a method needs a very accurate determination of the Hall coefficient as it does not depend on the mobilities in large B, see Eq. (A8). It is practical to estimate the mobilities from the fit to ρ_{xx} and use ρ_{xy} to confirm the legitimacy of the fit parameters.

In Fig. 6(b), we show the variation of the electron mobilities when the electron densities are varied for heterostructure 1. In both of the heterostructures, we find $\mu_2>\mu_1$.[18] It should be noted that the primary doping was performed at the side of the wide quantum well in our heterostructures. The large mobility for the excited-state subband is attributed to the screening of the ionized impurity potentials by the

electrons in the ground-state subband. When increasing the total electron density, μ_1 slightly decreases whereas μ_2 increases. The former is attributed to the increased number of ionized impurities. The latter is a consequence of the increase of the kinetic energy of the electrons in the excited-state subband. We have confirmed that the reverse situation $\mu_1 > \mu_2$ can be realized by increasing the spacer layer thickness for the principal doping from 10 nm to 30 nm. We obtain, for example, $\mu_1 = 179$ m^2/Vs and $\mu_2 = 10$ m^2/Vs when $n_1 = 3.7 \times 10^{15}$ m^{-2} and $n_2 = 0.9 \times 10^{15}$ m^{-2}.

[1] T. Ando, A.B. Fowler, and F. Stern, Rev. Mod. Phys. **54**, 437 (1982).

[2] T. Ando and Y. Uemura, J. Phys. Soc. Jpn. **37**, 1044 (1974).

[3] R.J. Nicholas, R.J. Haug, K. von Klitzing, and G. Weimann, Phys. Rev. B **37**, 1294 (1988).

[4] A. Usher, R.J. Nicholas, J.J. Harris, and C.T. Foxon, Phys. Rev. B **41**, 1129 (1990).

[5] Y. Guldner, J.P. Vieren, M. Voos, F. Delahaye, D. Dominguez, J.P. Hirtz, and M. Razeghi, Phys. Rev. B **33**, 3990 (1986).

[6] E.G. Gwinn, R.M. Westervelt, P.F. Hopkins, A.J. Rimberg, M. Sundaram, and A.C. Gossard, Phys. Rev. B **39**, 6260 (1989).

[7] H. van Houten, J.G. Williamson, M.E.I. Broekaart, C.T. Foxon, and J.J. Harris, Phys. Rev. B **37**, 2756 (1988).

[8] T.P. Smith III and F.F. Fang, Phys. Rev. B **37**, 4303 (1988).

[9] Y. Takagaki, K. Muraki, and S. Tarucha, Semicond. Sci. Technol. **13**, 296 (1998).

[10] Y. Takagaki and S. Tarucha, Semicond. Sci. Technol. **12**, 715 (1997).

[11] A.G. Davies, C.H.W. Barnes, K.R. Zolleis, J.T. Nicholls, M.Y. Simmons, and D.A. Ritchie, Phys. Rev. B **54**, 17 331 (1996).

[12] Y. Takagaki, K. Muraki, and S. Tarucha, Phys. Rev. B **56**, 1057 (1997).

[13] K. Ensslin, M. Sundaram, A. Wixforth, J.H. English, and A.C. Gossard, Phys. Rev. B **43**, 9988 (1991).

[14] D.G. Hayes, M.S. Skolnick, D.M. Whittaker, P.E. Simmonds, L.L. Taylor, S.J. Bass, and L. Eaves, Phys. Rev. B **44**, 3436 (1991).

[15] B. Tanatar and D.M. Ceperley, Phys. Rev. B **39**, 5005 (1989).

[16] M.M. Fogler and B.I. Shklovskii, Phys. Rev. B **52**, 17 366 (1995).

[17] R. A. Smith, *Semiconductors* (Cambridge University Press, Cambridge, England, 1961), Chap. 5.

[18] T.P. Smith III, F.F. Fang, U. Meirav, and M. Heiblum, Phys. Rev. B **38**, 12 744 (1988).